

## LHC Constraints on Scalar Diquarks

---

**Bruna Pascual-Dias,<sup>a</sup> Pratishruti Saha<sup>b</sup> and David London<sup>a</sup>**

<sup>a</sup>*Physique des Particules, Université de Montréal,  
C.P. 6128, succ. centre-ville, Montréal, QC, Canada H3C 3J7*

<sup>b</sup>*Harish-Chandra Research Institute, Chhatnag Road,  
Jhansi, Allahabad - 211019, India*

*E-mail:* [bruna.pascual.dias@umontreal.ca](mailto:bruna.pascual.dias@umontreal.ca), [pratishrutisaha@hri.res.in](mailto:pratishrutisaha@hri.res.in),  
[london@lps.umontreal.ca](mailto:london@lps.umontreal.ca)

**ABSTRACT:** A number of years ago, low-energy constraints on scalar diquarks, particles that couple to two quarks, were examined. It was found that the two most weakly-constrained diquarks are  $D^u$  and  $D^d$ , colour antitriplets that couple to  $u_R^i u_R^j$  and  $d_R^i d_R^j$ , respectively. These diquarks have not been observed at the LHC. In this paper, we add the LHC measurements to the low-energy analysis, and find that the constraints are significantly improved. As an example, denoting  $x^u$  as the  $D^u$  coupling to the first and second generations, for  $M_{D^u} = 600$  GeV, the low-energy constraint is  $|x^u| \leq 14.4$ , while the addition of the LHC dijet measurement leads to  $|x^u| \leq 0.13\text{--}0.15$ . Further improvements are obtained by adding the measurement of single top production with a  $p_T$  cut. These new constraints must be taken into account in making predictions for other low-energy indirect effects of diquarks.

---

## Contents

<b>1</b>	<b>Introduction</b>	<b>1</b>
<b>2</b>	<b>Scalar Diquarks</b>	<b>2</b>
<b>3</b>	<b>Low-energy Constraints</b>	<b>3</b>
<b>4</b>	<b>LHC Constraints: Direct Searches</b>	<b>5</b>
<b>5</b>	<b>LHC Constraints: Single Top Production</b>	<b>7</b>
<b>6</b>	<b>Conclusions</b>	<b>12</b>

---

## 1 Introduction

The Standard Model (SM) has been extremely successful in explaining almost all experimental measurements to date. However, for a variety of reasons – the hierarchy problem, dark matter, CP violation and the matter-antimatter asymmetry, etc. – it is generally believed that it is not complete. There must be physics beyond the SM. It was hoped that the LHC would produce new-physics (NP) particles directly, but so far this has unfortunately not happened. The scale of NP may be above the present reach of the LHC.

Still, even if this is the case, all hope is not lost: one can also search for NP through indirect signals. (Indeed, there are currently indirect hints of NP in  $b \rightarrow s\mu^+\mu^-$  and  $b \rightarrow c\tau^-\bar{\nu}_\tau$  transitions [1].) Of course, for a particular kind of NP, if one wants to examine how large the indirect effects can be in a given process, one must include the constraints on its mass and couplings derived from direct searches.

One possible type of NP is a diquark, a particle that couples to two quarks. A diquark can be a scalar or a vector, and transforms as a  $\mathbf{6}$  or  $\bar{\mathbf{3}}$  of  $SU(3)_C$ . In this paper, we focus on scalar diquarks. These appear in models with  $E_6$  [2] or  $SU(2)_L \times SU(2)_R \times SU(4)_C$  [3] symmetry, and in supersymmetry with R-parity violation [4]. Studies of diquark phenomenology mostly fall into three categories: (i) the LHC discovery reach for scalar diquarks [3, 5–19], (ii) explanations of the Tevatron  $t\bar{t}$  forward-backward asymmetry [20–28], and (iii) contributions to  $n$ - $\bar{n}$  oscillations [13, 29–35]. Thus, there is a good deal of room to examine the effect of diquarks in other processes (for example, see Refs. [36–38]).

In 2011, Giudice, Gripiaios and Sundrum (GGS) [39] considered diquarks with sizeable flavour-dependent couplings to light quarks, and examined the low-energy constraints<sup>1</sup> from flavour-changing neutral currents, electric-dipole moments and neutral meson mixing. This was done for both the  $\mathbf{6}$  and  $\bar{\mathbf{3}}$  diquarks. They found that two types of diquark, both

---

<sup>1</sup>Other analyses have examined the constraints on diquarks from LEP data [40] and flavour physics [41].

transforming as a  $\bar{\mathbf{3}}$  under  $SU(3)_C$ , were rather immune to the constraints. That is, they could be rather light even while keeping reasonably large couplings. They are  $D^u$  and  $D^d$ , diquarks that couple to  $u_R^i u_R^j$  and  $d_R^i d_R^j$ , respectively (here  $i$  and  $j$  are generation indices). They encouraged the search for these scalar diquarks at the LHC.

Now, we know that, to date, diquarks have not been observed at the LHC. But this does not exclude the possibility of measurable indirect effects in low-energy processes. As noted above, if one wants to predict how large such effects can be in a particular process, it is important to take into account the constraints from direct searches on the diquark's mass and couplings.

With this in mind, in this paper we extend the GGS analysis to include the constraints from the LHC. These come in two types. First, there are the constraints from direct searches, which apply to both  $D^u$  and  $D^d$ . Second, there are indirect constraints on  $D^u$  due to its contribution to top-quark production. Processes that can potentially be important include the production of  $t\bar{t}$ ,  $tt$  and single top production. We will show that the LHC constraints reduce the allowed parameter space of diquark masses and couplings compared to GGS.

We begin in Sec. 2 with a summary of the various scalar diquarks. The low-energy (GGS) constraints are reviewed in Sec. 3. Sec. 4 contains our analysis of the constraints from direct searches at the LHC. Constraints from single top production are examined in Sec. 5. We conclude in Sec. 6.

## 2 Scalar Diquarks

We consider the addition of a scalar diquark to the SM. This scalar diquark  $D$  has mass  $M_D$ , spin 0, and couples to a pair of quarks. Similar to the parametrization of Ref. [9], we write the interaction Lagrangian after electroweak symmetry breaking as

$$\mathcal{L} = \sqrt{2} \bar{K}_k^{ab} D^k \bar{q}_a^i \lambda_{ij} P_{L,R} q_b^{jC} + \text{h.c.} \quad (2.1)$$

Here  $a, b \in \{1, 2, 3\}$  are colour indices,  $i, j \in \{1, 2, 3\}$  are generation indices,  $P_{L,R} \equiv (1 \mp \gamma^5)/2$  is the left- or right-chirality projection operator, and  $q^C \equiv C \bar{q}^T$  is the conjugate quark field. Since it couples to two quarks, the diquark  $D^k$  transforms as a  $\mathbf{6}$  or  $\bar{\mathbf{3}}$  of  $SU(3)_C$ ; the index  $k$  runs over the components of the representation (1 to 6 for a  $\mathbf{6}$ , 1 to 3 for a  $\bar{\mathbf{3}}$ ). The  $\bar{K}_k^{ab}$  are the  $SU(3)_C$  Clebsch-Gordan coefficients coupling this representation to two  $\mathbf{3}$ s.  $\lambda_{ij}$  is the coupling to the  $i$  and  $j$  generations. Note that the two quarks coupling to the diquark have the same chirality.

The Clebsch-Gordan coefficients  $K_{ab}^k$  for the  $\mathbf{6}$  diquark representation are symmetric, while for the  $\bar{\mathbf{3}}$  diquark representation the  $K_{ab}^k$  are antisymmetric. Given that a  $\bar{\mathbf{3}}$  diquark is an antifundamental representation of  $SU(3)_C$  [9], we can assign it a single colour index  $c$ . This allows us to write the Lagrangian for a  $\bar{\mathbf{3}}$  diquark as

$$\mathcal{L}^{\bar{\mathbf{3}}} = \epsilon^{cab} D_c \bar{q}_a^i \lambda_{ij} P_{L,R} q_b^{jC} + \text{h.c.} \quad (2.2)$$

When two quarks combine to form a diquark, the symmetry of the combined state is directly dependent on the individual symmetries under  $SU(3)_C$  and  $SU(2)_L$ . For instance,

Name	$SU(3)_C$	$SU(2)_L$	$U(1)_Y$	Coupling
I	<b>6</b>	<b>3</b>	+1/3	$(Q_L Q_L)$
II	$\bar{\mathbf{3}}$	<b>3</b>	+1/3	$[Q_L Q_L]$
III	<b>6</b>	<b>1</b>	+1/3	$[Q_L Q_L], u_R d_R$
IV	$\bar{\mathbf{3}}$	<b>1</b>	+1/3	$(Q_L Q_L), u_R d_R$
V	<b>6</b>	<b>1</b>	+4/3	$(u_R u_R)$
VI $\equiv D^u$	$\bar{\mathbf{3}}$	<b>1</b>	+4/3	$[u_R u_R]$
VII	<b>6</b>	<b>1</b>	-2/3	$(d_R d_R)$
VIII $\equiv D^d$	$\bar{\mathbf{3}}$	<b>1</b>	-2/3	$[d_R d_R]$

**Table 1.** Scalar diquarks classified by their charges under the SM gauge group. In the ‘Coupling’ column, parentheses indicate a symmetric coupling and square brackets indicate an antisymmetric coupling with respect to flavour indices [39].

consider  $Q_L Q_L$ . Under  $SU(3)_C$ , the combination of two **3**s produces a **6** (symmetric) and a  $\bar{\mathbf{3}}$  (antisymmetric). Under  $SU(2)_L$ ,  $\mathbf{2} \times \mathbf{2}$  yields a **3** (symmetric) and a **1** (antisymmetric). Thus, the state  $(\bar{\mathbf{3}}, \mathbf{1})_{+1/3}$  of  $SU(3)_C \times SU(2)_L$  is overall symmetric. Similarly, if one considers  $u_R u_R$ , the state  $(\bar{\mathbf{3}}, \mathbf{1})_{+4/3}$  is antisymmetric.

The symmetry of the combined state under interchange of quarks has important implications for the couplings of the diquark. If the diquark state is antisymmetric under the exchange of two quarks, then the coupling to two quarks of the same flavour vanishes. As a consequence, we see that the antisymmetric diquarks only couple to pairs of quarks with different flavours. We thus see that the antisymmetry of the diquark state under the SM gauge group entails an antisymmetry under flavour [39]. This antisymmetry has important consequences, as it implies that any flavour-changing diagram must involve all three generations of quarks [39].

With this in mind, all possible scalar diquarks that couple to quarks within the SM can be classified by their charges under the SM gauge group  $SU(3)_C \times SU(2)_L \times U(1)_Y$  [12, 39]. They are presented in Table 1, where we use the convention  $Q = I_3 + Y$ .

### 3 Low-energy Constraints

In Ref. [39], GGS worked out the low-energy constraints on these diquarks. We review their results in this section.

First, if one imposes only the  $SU(3)_C \times SU(2)_L \times U(1)_Y$  gauge symmetry, diquarks can also have a dimension-four Yukawa-type coupling to a lepton and a quark [42]. The presence of both diquark and leptoquark couplings would lead to proton decay [39], and would of course place extremely stringent constraints on the diquarks’ couplings and masses. This would essentially rule out any effects at the TeV scale and below. In order to avoid this, there must be an additional global symmetry, such as lepton number or baryon number, that forbids this leptoquark coupling.

Diquarks I, V and VII all contribute at tree level to the  $\Delta F = 2$  process  $M^0 - \bar{M}^0$  mixing ( $M = K, D, B_d, B_s$ ) (see Fig. 1a). This leads to very strong constraints on these

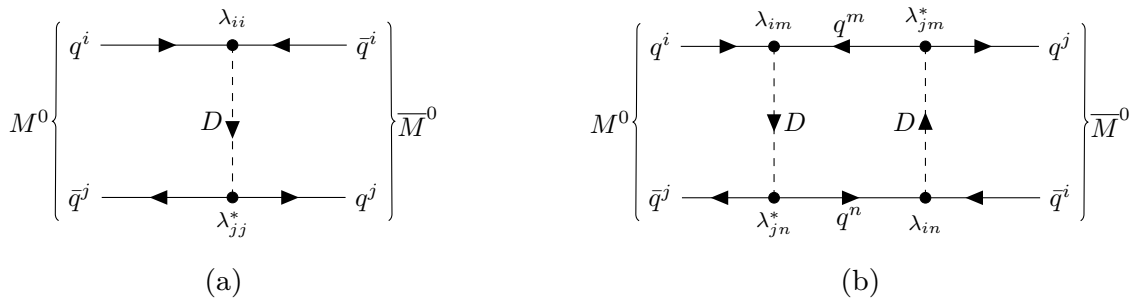


**Figure 1.** Diquark contributions to  $M^0$ - $\bar{M}^0$  mixing at (a) tree level and (b) one loop.

diquarks. The other diquarks contribute to meson mixing at one loop via a box diagram (see Fig. 1b). However, not all contributions are the same size. Consider diquark II. Since it couples only to left-handed quarks, there is also a box diagram in which one of the internal diquarks is replaced by a  $W$ . And since the  $W$  is considerably lighter than the  $D$ , this amplitude is larger than the analogous amplitude with two virtual diquarks, leading to stronger constraints on diquark II. As for diquarks III and IV, they couple to both left- and right-handed  $u^i d^j$  pairs. This leads to non-chiral  $\Delta F = 2$  operators which are greatly enhanced when compared to the chiral operators. Once again, this leads to stronger constraints on diquarks III and IV. This result holds even in the case where one of the couplings (left- or right-handed) dominates [39].

The upshot is that, of the eight possible diquarks, two of them – VI  $\equiv D^u$  and VIII  $\equiv D^d$  – are more weakly constrained than the others. It is for this reason that GGS suggested that these scalar diquarks be searched for at the LHC. In this paper, we examine the additional constraints on these diquarks from the LHC using direct searches and measurements of top production.

The  $D^q$  diquark ( $q = u, d$ ) couples to  $q_R^i q_R^j$ . Since it transforms as  $(\bar{\mathbf{3}}, \mathbf{1})$  under  $SU(3)_C \times SU(2)_L$ , the coupling  $\lambda_{ij}$  is antisymmetric. In their analysis, GGS write this coupling as

$$\lambda_{ij}^q \equiv \epsilon_{ijk} \lambda_k^q \quad \Longrightarrow \quad \lambda^q = \begin{pmatrix} 0 & \lambda_3^q & -\lambda_2^q \\ -\lambda_3^q & 0 & \lambda_1^q \\ \lambda_2^q & -\lambda_1^q & 0 \end{pmatrix}. \quad (3.1)$$

The constraints on the  $\lambda_i^q$  come from a variety of processes. For real couplings, which we consider in our analysis, they are as follows. For  $\lambda_i^d$ , they include  $K^0$ - $\bar{K}^0$  and  $B_d^0$ - $\bar{B}_d^0$  mixing,  $b \rightarrow s\gamma$  and  $b \rightarrow d\gamma$ ,  $R_b$ , and  $B^\pm \rightarrow \phi\pi^\pm$ . For  $\lambda_i^u$ , there are only  $D^0$ - $\bar{D}^0$  mixing and  $A_c$  (defined in terms of the coupling of the  $Z$  boson to charm quarks). The constraints from these various quantities are given in Table 2.

In our analysis, we distinguish between the couplings that involve only light quarks (first and second generations) and those involving the third generation of quarks (we assume the couplings involving the first and third generations have the same magnitude as those involving the second and third generations). In the GGS convention, this corresponds to

Process	Bound ( $M_D/\text{TeV}$ )
$\Delta m_K$	$ \lambda_1^d \lambda_2^d  \leq 4.6 \times 10^{-2}$
$B_d^0-\bar{B}_d^0$ mixing	$ \lambda_1^d \lambda_3^d  \leq 3.6 \times 10^{-2}$
$b \rightarrow s\gamma$	$\sqrt{ \lambda_2^d \lambda_3^d } \leq 1.8$
$b \rightarrow d\gamma$	$\sqrt{ \lambda_1^d \lambda_3^d } \leq 0.9$
$R_b$	$ \lambda_{1,2}^d  \leq 24$
$B^\pm \rightarrow \phi\pi^\pm$	$\sqrt{ \lambda_1^d \lambda_3^d } \leq 0.1$
$D^0-\bar{D}^0$ mixing	$ \lambda_1^u \lambda_2^u  \leq 1.5 \times 10^{-2}$
$A_c$	$ \lambda_3^u  \leq 24$

**Table 2.** Bounds in units of  $M_D/\text{TeV}$  on the couplings of the diquarks  $D^d$  and  $D^u$  [39].

setting  $\lambda_1^q = \lambda_2^q = y^q$  and  $\lambda_3^q = x^q$ . The coupling matrix is then given by

$$\lambda^q = \begin{pmatrix} 0 & x^q & -y^q \\ -x^q & 0 & y^q \\ y^q & -y^q & 0 \end{pmatrix}. \quad (3.2)$$

We can now translate the GGS bounds to our notation. For  $D^u$ , the bound from  $D^0-\bar{D}^0$  mixing yields  $|y^u|^2 \leq 1.5 \times 10^{-2} (M_D/\text{TeV})$ , or  $|y^u| \leq 0.12 \sqrt{(M_D/\text{TeV})}$ . The bound from the electroweak precision tests ( $A_c$ ) is  $|x^u| \leq 24 (M_D/\text{TeV})$ . For  $D^d$ , the  $K^0-\bar{K}^0$  mass difference  $\Delta m_K$  imposes that  $|y^d| \leq \sqrt{4.6 \times 10^{-2} (M_D/\text{TeV})}$ . Similarly, the constraints from  $B_d^0-\bar{B}_d^0$  mixing require  $|x^d y^d| \leq 3.6 \times 10^{-2} (M_D/\text{TeV})$ .

In our analysis, we consider two diquark masses,  $M_D = 600 \text{ GeV}$  and  $M_D = 1 \text{ TeV}$ . For these two masses, the constraints are<sup>2</sup>

$$\begin{array}{ll} M_D = 600 \text{ GeV} & M_D = 1 \text{ TeV} \\ |y^u| \leq 0.09, & |y^u| \leq 0.12, \\ |x^u| \leq 14.4, & |x^u| \leq 24, \\ |y^d| \leq 0.17, & |y^d| \leq 0.21, \\ |x^d y^d| \leq 0.022, & |x^d y^d| \leq 0.036. \end{array} \quad (3.3)$$

#### 4 LHC Constraints: Direct Searches

In this section, we obtain constraints on the diquark parameter space using measurements of dijet production at the LHC. In Ref. [43], the CMS Collaboration presents measurements of narrow dijet resonances at  $\sqrt{s} = 13 \text{ TeV}$ . It is found that the data exclude the scalar diquarks in  $E_6$  models [2] with a coupling constant of electromagnetic strength for masses less than 7.2 TeV. This result is obtained from the model-independent observed 95% CL

<sup>2</sup>For  $|x^d y^d|$ , we consider the constraint from  $B_d^0-\bar{B}_d^0$  mixing, as the constraint from  $B^\pm \rightarrow \phi\pi^\pm$ , though apparently more stringent, involves additional theoretical assumptions [39].

upper limits on the product  $\sigma BA$  for quark-quark resonances. Here  $\sigma$  is the production cross section,  $B$  is the branching ratio for a dijet decay, and  $A$  is the acceptance, which includes kinematic requirements of the dijet final state. The observed and expected values of  $\sigma BA$  from Ref. [43] are presented in Fig. 2 as black dots and a red dashed line, respectively. Ref. [43] states that these limits can be directly compared to parton-level calculations of  $\sigma BA$  without detector simulation.

In order to get constraints from direct searches, we compare these results with the predictions of  $\sigma BA$  for the scalar diquarks  $D^u$  and  $D^d$ . These are obtained by calculating the leading-order (LO) cross section for the production process  $pp \rightarrow D^{u,d}$ , as well as the branching ratio for the decay of the corresponding diquark into light quarks, namely  $BR(D^u \rightarrow uc)$  and  $BR(D^d \rightarrow ds)$ . The acceptance is calculated following the prescription in Ref. [43]. It is defined as  $A = A_\Delta A_\eta$ , where  $A_\Delta$  is the acceptance of requiring  $|\Delta\eta| < 1.3$  for the dijet system and  $A_\eta$  is the acceptance of also requiring  $|\eta| < 2.5$  for each of the jets. Since we are considering scalar diquarks, which have isotropic decays, we set  $A_\Delta = 0.57$  for all masses. For diquark masses less than 1.6 TeV, we set  $A_\eta = 0.95$  to account for the decrease of acceptance in this lower mass range. For larger masses,  $A_\eta$  is set to 1. In summary, the acceptance for the low-mass range is set to  $A = 0.54$  while for higher masses it is set to  $A = 0.57$ .

The calculations are performed using MadGraph5\_amc@NLO version 2.7.2 [44] by implementing the NP alongside the SM with FeynRules [45]. We base our implementation on the existing model file for triplet diquarks in the FeynRules model database [46]. The parton distribution function (PDF) used is CTEQ6L1 [47] and both the renormalization and factorization scales are set to the diquark mass  $M_D$ . The LO cross section calculated by MadGraph5\_amc@NLO is multiplied by an approximate NLO  $K$  factor ( $K = 1.3$ ) based on the results of Ref. [9]. In all calculations, the requirements for the narrow-width approximation are satisfied: the  $\Gamma/M_D$  ratio is smaller than 2% for couplings up to 0.2 and it is smaller than 5% for couplings up to 0.3.

We begin by considering the case where all the diquark couplings are equal and of electromagnetic strength,  $\lambda_{ij} = 0.3$ , for masses ranging from 600 GeV to 8.1 TeV. The predicted values of  $\sigma BA$  for both diquarks are presented in Fig. 2. We find the lower bounds on the masses to be  $M_{D^u}, M_{D^d} \gtrsim 2.5$  TeV. The limits are nearly identical for  $D^u$  and  $D^d$ . This is expected. For each diquark, the production is dominated by one subprocess:  $uc \rightarrow D^u$  and  $ds \rightarrow D^d$ . At the same time, the relative densities of the initial-state quarks inside the proton roughly follow the order  $u > d > s > c$ . The combination of the two effects means that the predictions for  $\sigma BA$  are very similar in the two cases. The differences become more pronounced as we go to higher diquark masses.

Next, we explore the scenario where the light-quark couplings  $x^q$  and the third-generation couplings  $y^q$  are different. We consider two representative diquark masses of 600 GeV and 1 TeV, and perform a scan over the pair of couplings  $(x^q, y^q)$ , in which each coupling varies from 0.05 to 0.3 in steps of 0.01. For each pair, we calculate the corresponding prediction for  $\sigma BA$ . A cubic interpolation is then performed in order to span the entire region of interest in the parameter space. The resulting values are compared to the observed upper limits obtained by CMS. It must be noted that, for coupling values

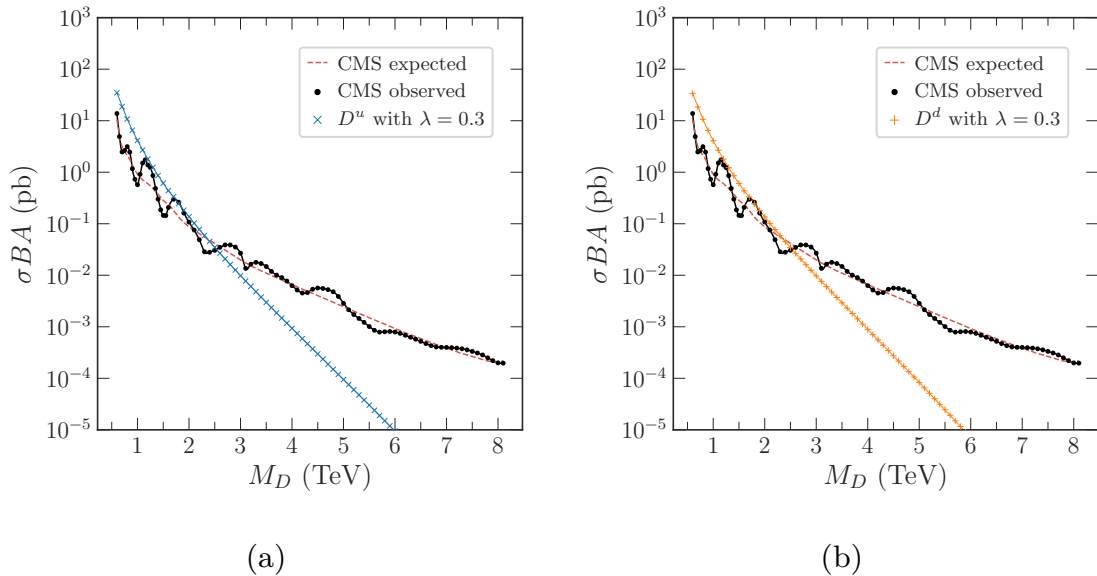


**Figure 2.** Theoretical predictions of  $\sigma BA$  for diquarks  $D^u$  (blue cross) and  $D^d$  (orange plus sign), for the case where all couplings are equal and of electromagnetic strength. Observed values at 95% CL (black dots) and expected values (red dashed line) from Ref. [43] are presented for comparison.

lower than 0.05, the calculated partial width of the diquark is smaller than the QCD scale, meaning that a perturbative approach is no longer valid. For this reason we do not consider couplings less than 0.05.

The  $\sigma BA$  predictions for  $D^u$  can be found in Fig. 3. We superpose the bounds from GGS [Eq. (3.3)] (black dashed line). The region of parameter space above this line is excluded. We draw the bound on  $\sigma BA$  from CMS (red solid line), so the region to the right of this line (dark shade of red) is excluded and the region to the left (light shade of red) is allowed. The net effect is that there is a considerable improvement over the GGS bounds. Specifically, there are new constraints on the coupling to lighter generations,  $|x^u|$ . For  $M_{D^u} = 600$  GeV,  $|x^u|$  must take values less than 0.13–0.15, while, for  $M_{D^u} = 1$  TeV, this upper limit is 0.08–0.11. In both cases, the value of the upper limit on  $|x^u|$  depends on the value of  $|y^u|$ .

For  $D^d$ , the  $\sigma BA$  predictions are shown in Fig. 4. The GGS bounds [Eq. (3.3)] on  $|x^d y^d|$  (black dashed line) and  $|y^d|$  (black dotted line) are superposed, as is the  $\sigma BA$  bound from CMS (red solid line). As above, the region to the right of this red solid line is excluded and the region to the left is allowed. Once again, we find a significant improvement over the GGS bounds:  $|x^d| \leq 0.15$ –0.17 ( $M_{D^d} = 600$  GeV) and 0.09–0.13 ( $M_{D^d} = 1$  TeV).

## 5 LHC Constraints: Single Top Production

Further LHC constraints on diquarks can come from measurements of top-quark production. Processes potentially include the production of  $t\bar{t}$  pairs,  $t\bar{t}$  pairs, and single top

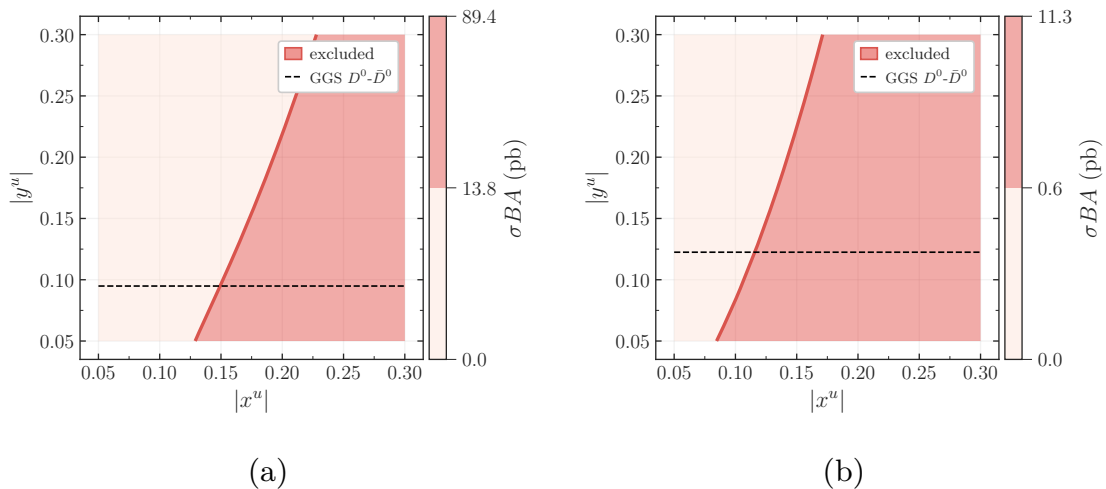


**Figure 3.** Theoretical predictions of  $\sigma BA$  for the  $D^u$  diquark with (a)  $M_{D^u} = 600$  GeV and (b)  $M_{D^u} = 1$  TeV for different values of the light-quark coupling  $|x^u|$  and the third-generation coupling  $|y^u|$ . The observed 95% CL upper limit on  $\sigma BA$  [43] is indicated by the red solid line. The black dashed line denotes the GGS constraint on  $|y^u|$  [Eq. (3.3)].

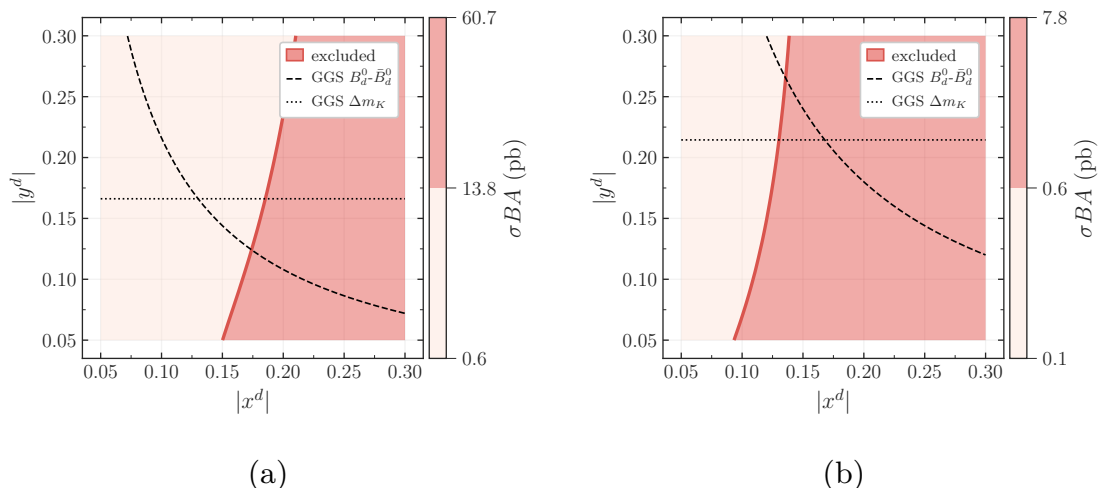


**Figure 4.** Theoretical predictions of  $\sigma BA$  for the  $D^d$  diquark (a)  $M_{D^d} = 600$  GeV and (b)  $M_{D^d} = 1$  TeV, for different values of the light-quark coupling  $|x^d|$  and the third-generation coupling  $|y^d|$ . The observed 95% CL upper limit on  $\sigma BA$  [43] is indicated by the red solid line. The black dashed line and black dotted line denote the GGS constraints on  $|x^d y^d|$  and  $|y^d|$ , respectively [Eq. (3.3)].

production. These constraints are explored in this section. Note that here we are interested in obtaining an improvement over the constraints already obtained from the dijet channel.

Two points are immediately obvious. First, only the  $D^u$  diquark can contribute to

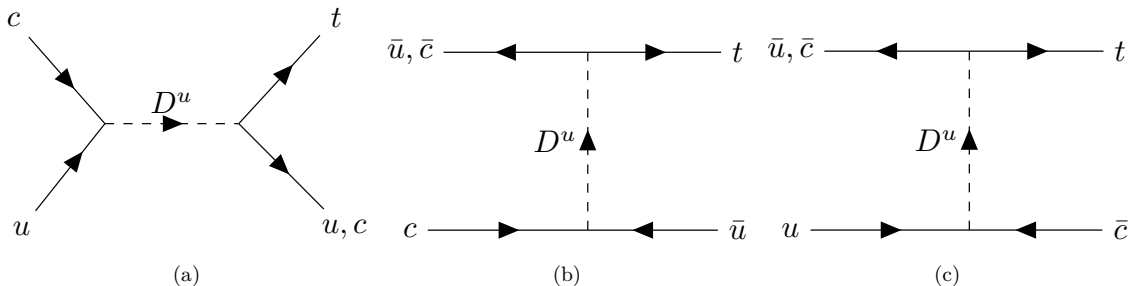


**Figure 5.** Diquark contributions to single-top production in the  $t$  channel in  $pp$  collisions.

these processes since the  $D^d$  diquark does not couple to top quarks. Thus, any constraints apply only to  $D^u$ . Second, because this diquark is an antisymmetric state, it cannot couple to two quarks of the same flavour. As a result, it does not contribute to  $tt$  production. This leaves us with  $t\bar{t}$  and single top production.

Consider first the production of  $t\bar{t}$  pairs. At the LHC, its cross-section is dominated by gluon-initiated processes. The remaining contributions arise from  $q\bar{q} \rightarrow t\bar{t}$  processes, which would include contributions from the  $D^u$  diquark. However, if we restrict to couplings allowed by the GGS and dijet data, we find that the diquark contribution is overwhelmed by the SM contributions. For this reason, we are not able to obtain meaningful constraints from  $t\bar{t}$  production measurements.

We now turn to single-top production (STP) [48]. In the SM, this process occurs at LO via three modes: a  $t$ -channel process  $q\bar{b} \rightarrow q't$  and an  $s$ -channel process  $q\bar{q}' \rightarrow t\bar{b}$ , both occurring through  $W$ -boson exchange, and a direct  $tW$  production. Of these, the dominant production mechanism at the LHC is via the  $t$ -channel. Indeed, this has been measured by both the ATLAS and the CMS Collaborations with greater precision than the other modes. Now, the  $D^u$  diquark can contribute at tree level to this STP mode, as shown in Fig. 5. Thus, by comparing the measured value of the cross section for this process with the predicted value including both the SM and NP, it is possible to put further constraints on the mass and couplings of the  $D^u$  diquark.

A summary of the measurements of the STP cross sections at the LHC is shown in Fig. 6. For the combined productions of  $t$  and  $\bar{t}$  quarks in the  $t$  channel, we have the following measurements:  $\sigma(tq + \bar{t}q) = 89.6^{+7.1}_{-6.3}$  pb for  $\sqrt{s} = 8$  TeV from ATLAS [49] and  $\sigma(tq + \bar{t}q) = 207 \pm 31$  pb for  $\sqrt{s} = 13$  TeV from CMS [50]. These must be compared to the SM prediction. The SM prediction of the  $t$ -channel STP cross section for  $pp$  collisions recommended by the ATLAS and CMS Collaborations [52] is  $\sigma_{\text{SM}}(tq + \bar{t}q) = 84.7^{+3.8}_{-3.2}$  pb at  $\sqrt{s} = 8$  TeV and  $\sigma_{\text{SM}}(tq + \bar{t}q) = 217^{+9.0}_{-7.7}$  pb at  $\sqrt{s} = 13$  TeV. These are calculated for  $m_t = 172.5$  GeV at next-to-leading order (NLO) in QCD using Hathor v2.1 [53, 54]. The PDF and  $\alpha_S$  uncertainties are calculated using the PDF4LHC prescription [55] with the MSTW2008 68% CL NLO [56, 57], CT10 NLO [58] and NNPDF2.3 [59] PDF sets, added in quadrature to the scale uncertainty [52].

In order to put constraints on the  $D^u$  diquark, we calculate the LO cross section  $\sigma_{LO}(tq + \bar{t}q)$  for the production of a  $t$  or  $\bar{t}$  accompanied by a light quark from a  $pp$  collision.

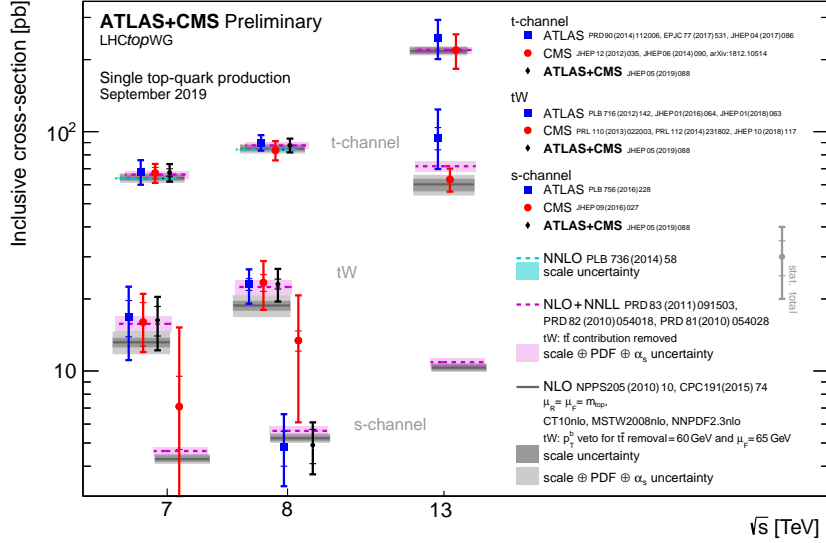


**Figure 6.** Summary of the available single-top production cross-section measurements from the LHC [51].

These calculations are once again performed using MadGraph5\_amc@NLO version 2.7.2 [44] by implementing the NP alongside the SM with FeynRules [45]. We use the CTEQ6L1 PDF [47] and both the renormalization and factorization scales are set to  $m_t = 173$  GeV. In order to approximate higher-order QCD corrections, this value is then scaled with the corresponding  $K$  factors obtained from the NLO SM predictions,  $K = \sigma_{\text{NLO}}^{\text{SM}}/\sigma_{\text{LO}}^{\text{SM}}$ , which are  $K = 1.13$  for  $\sqrt{s} = 8$  TeV and  $K = 1.12$  for  $\sqrt{s} = 13$  TeV. In our analysis, we consider diquark masses of 600 GeV and 1 TeV, and we scan over the pair of couplings  $(x^u, y^u)$ , in which each coupling varies from 0.05 to 0.3 in steps of 0.05. Moreover, a cubic interpolation is performed in order to span the region of interest in the parameter space and to draw filled contour plots.

The predictions for the  $t$ -channel STP cross section at  $\sqrt{s} = 8$  TeV and 13 TeV, for  $M_{D^u} = 600$  GeV are shown in Fig. 7. The corresponding experimental measurement is drawn, as are the boundaries of the regions describing the  $1\sigma$ ,  $2\sigma$  and  $3\sigma$  deviations from the experimental central value. Constraints from GGS and from the direct searches described in Sec. 4 are also shown. We see that, at this stage, STP measurements do not lead to an improvement over the previously-obtained constraints, *i.e.*, those from GGS and dijet measurements. In fact, for  $M_{D^u} = 1$  TeV, the predictions for  $\sigma(tq + \bar{t}q)$  lie entirely within the  $1\sigma$  region of the measurement, for all  $|x^u|$  and  $|y^u|$  considered. For this reason we do not include those plots here.

In order to improve upon the earlier constraints, we focus on a reduced phase space. To be specific, we consider two  $p_T$  intervals:  $50 \text{ GeV} \leq p_T(t) \leq 300 \text{ GeV}$  and  $100 \text{ GeV} \leq p_T(t) \leq 300 \text{ GeV}$ . While these cuts can be easily implemented in MadGraph5\_amc@NLO to obtain the theory SM+NP prediction, the corresponding measurements are not readily available. We use measurements of the differential cross section from ATLAS [49] at  $\sqrt{s} = 8$  TeV and integrate over a subset of the bins to obtain both the experimental central

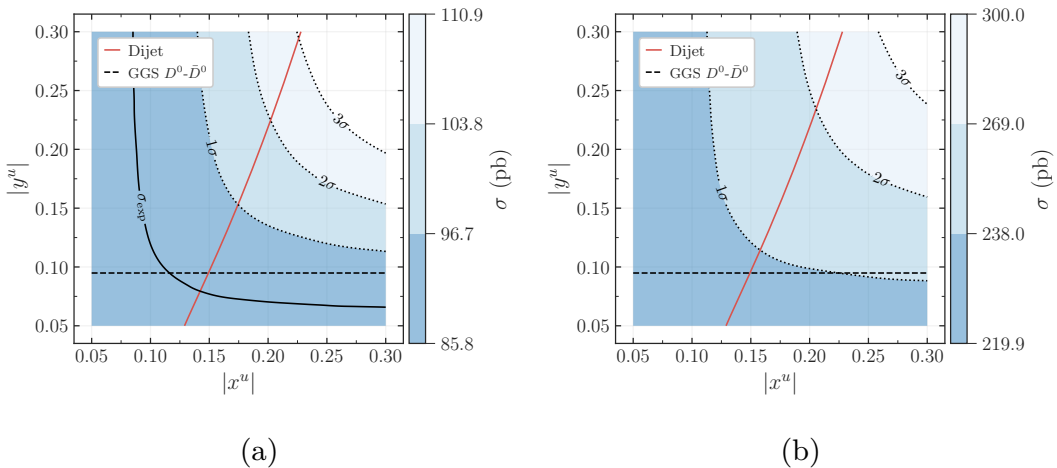


**Figure 7.** Theoretical predictions of the total STP cross section  $\sigma$  including the contributions of the diquark  $D^u$ . Results are shown for  $M_{D^u} = 600$  GeV at (a)  $\sqrt{s} = 8$  TeV and (b)  $\sqrt{s} = 13$  TeV. The central value  $\sigma_{\text{exp}}$  of the experimental measurement is shown (black solid line), as are the  $1\sigma$ ,  $2\sigma$  and  $3\sigma$  regions (black dotted lines). Constraints from  $D^0$ - $\bar{D}^0$  mixing (black dashed line) [39] and direct searches (red solid line) (Sec. 4) are also included.

value and the uncertainties for each range of  $p_T(t)$ . We obtain  $47.7 \pm 2.5$  pb for the interval starting at 50 GeV and  $16.1 \pm 1.5$  pb for the one starting at 100 GeV. Furthermore, as our calculation in MadGraph5\_amc@NLO is at LO, we need to obtain appropriate  $K$  factors to approximate the NLO contribution. We do this by carrying out the same integration procedure, this time on the SM prediction in the ATLAS analysis [49, 60]. Our LO results are then scaled up using  $K$  factors, namely  $K = 1.33$  for the interval starting at 50 GeV and  $K = 1.53$  for the interval starting at 100 GeV.

The theoretical predictions for the total STP cross section with  $M_{D^u} = 600$  GeV and the aforementioned cuts on  $p_T(t)$  are shown in Fig. 8. We have varied  $(x^u, y^u)$  from 0.05 to 0.2 in steps of 0.01. We now observe a reduction of the allowed region of coupling values compared to the allowed regions from the previously-discussed constraints. These results indicate that the consideration of cuts can indeed strengthen the constraints on the  $D^u$  diquark.

A similar analysis can be performed for  $M_{D^u} = 1$  TeV. However, in order to obtain an improvement on the constraints, one would have to choose a different  $p_T$  interval, excluding more of the lower  $p_T$  region and including more of the higher  $p_T$  region. That is, measurements of the differential cross section up to higher values of  $p_T$  would be required. These are as yet unavailable. If they do become available in the future, for  $\sqrt{s} = 8$  TeV and/or 13 TeV, it would be possible to obtain more stringent constraints on diquarks of masses 1 TeV and higher.

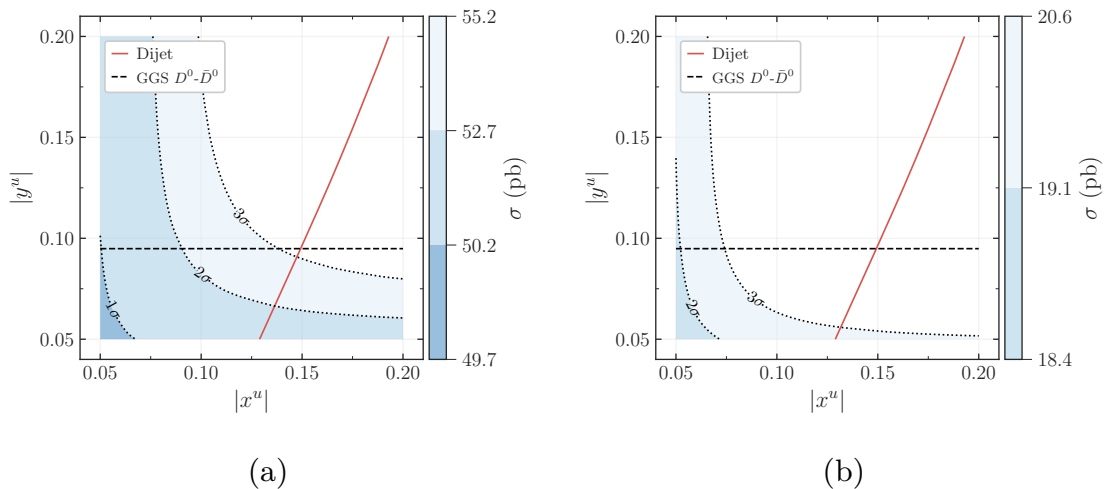


**Figure 8.** Theoretical predictions of the total STP cross section  $\sigma$  at  $\sqrt{s} = 8$  TeV including the contributions of the diquark  $D^u$  with  $M_{D^u} = 600$  GeV. Results are shown for different top transverse momentum  $p_T(t)$  intervals, where the minimum values for  $p_T(t)$  are (a) 50 GeV and (b) 100 GeV, both having a maximum value of 300 GeV. The central value  $\sigma_{\text{exp}}$  of the experimental measurement is shown (black solid line), as are the  $1\sigma$ ,  $2\sigma$  and  $3\sigma$  regions (black dotted lines). Constraints from  $D^0$ - $\bar{D}^0$  mixing (black dashed line) [39] and direct searches (red solid line) from Sec. 4 are also included.

## 6 Conclusions

For a variety of reasons, it is generally believed that there must be physics beyond the SM. The clearest evidence of this NP would be if new particles were produced at high-energy colliders. Unfortunately, to date, direct searches at the LHC have not found any evidence of new particles. The other way of finding NP is through indirect searches: if the measurement of a low-energy process disagreed with the SM prediction, that would indicate the presence of NP. Suppose that such an indirect signal were seen. In order to check if a particular type of NP could be responsible, it would be necessary to (i) determine what mass and couplings of the NP particle are required to explain the indirect signal, and (ii) check whether such values of the mass and couplings are consistent with constraints from direct searches. In other words, as part of the program of indirect searches for NP, it is important to keep track of the direct-search constraints.

In this paper, we apply this to scalar diquarks, particles that couple to two quarks. There are eight different types of scalar diquarks. In Ref. [39], Giudice, Gripaio and Sundrum (GGS) found that the two most weakly-constrained diquarks are  $D^u$  and  $D^d$ , which both transform as a  $\bar{\mathbf{3}}$  under  $SU(3)_C$ , and couple respectively to  $u_R^i u_R^j$  and  $d_R^i d_R^j$ . To date, these diquarks have not been observed at the LHC. We therefore extend the GGS analysis to include the constraints from the LHC, focusing on two masses:  $M_D = 600$  GeV and 1 TeV.

There are two types of LHC constraints. First, there are the measurements by the

CMS Collaboration of narrow dijet resonances at  $\sqrt{s} = 13$  TeV [43] which apply to both  $D^u$  and  $D^d$ . We find that these measurements provide significant improvements on the GGS constraints. Here are some examples. We denote  $x^q$  as the  $D^q$  coupling to the first and second generations, and  $y^q$  as the  $D^q$  couplings to the first and third or second and third generations. For  $M_D = 600$  GeV, GGS finds  $|x^u| \leq 14.4$  and  $|x^d y^d| \leq 0.022$  (with  $|y^d| \leq 0.17$ ). The LHC dijet constraints imply  $|x^u| \leq 0.13\text{--}0.15$  and  $|x^d| \leq 0.15\text{--}0.17$ .

The second constraint applies only to  $D^u$ , and arises from its indirect contribution to single top production. We find that, using only the cross section measurements (Fig. 6), there are no improvements on the above constraints. However, for  $M_D = 600$  GeV, we find that the allowed region of  $(|x^u|, |y^u|)$  parameter space can be significantly reduced by applying a  $p_T$  cut.

Finally, the reader may have wondered why we chose diquark masses of 600 GeV and 1 TeV for our detailed analysis. So far, we have not addressed/explained this choice. On the other hand, by now it may have already become clear: our purpose was to demonstrate how the constraints on the diquark parameter space can be improved using data from dijet and STP measurements. We chose diquark masses for which this demonstration was possible with the existing experimental data. The LHC will run for several more years, and additional data, particularly for STP in the high  $p_T$  region, can be used in the future to improve and extend the limits obtained here.

**Acknowledgments:** We thank J.-F. Arguin for useful discussions. This work was financially supported by NSERC of Canada (BPD, DL). The work of PS was supported by the Department of Science and Technology, India, under the INSPIRE Faculty Scheme Grant No. IFA14-PH-105.

## References

- [1] For a review, see D. London, “Anomalies in B Decays: A Sign of New Physics?,” [arXiv:1911.06238 [hep-ph]].
- [2] J. L. Hewett and T. G. Rizzo, “Low-Energy Phenomenology of Superstring Inspired  $E_6$  Models,” Phys. Rept. **183**, 193 (1989). doi:10.1016/0370-1573(89)90071-9
- [3] R. N. Mohapatra, N. Okada and H. B. Yu, “Diquark Higgs at LHC,” Phys. Rev. D **77**, 011701 (2008) doi:10.1103/PhysRevD.77.011701 [arXiv:0709.1486 [hep-ph]].
- [4] R. Barbier, C. Berat, M. Besancon, M. Chemtob, A. Deandrea, E. Dudas, P. Fayet, S. Lavignac, G. Moreau, E. Perez and Y. Sirois, “R-parity violating supersymmetry,” Phys. Rept. **420**, 1-202 (2005) doi:10.1016/j.physrep.2005.08.006 [arXiv:hep-ph/0406039 [hep-ph]].
- [5] H. Tanaka and I. Watanabe, “Color sextet quark productions at hadron colliders,” Int. J. Mod. Phys. A **7**, 2679 (1992). doi:10.1142/S0217751X92001204
- [6] S. Atag, O. Cakir and S. Sultansoy, “Resonance production of diquarks at the CERN LHC,” Phys. Rev. D **59**, 015008 (1999). doi:10.1103/PhysRevD.59.015008
- [7] O. Cakir and M. Sahin, “Resonant production of diquarks at high energy  $pp$ ,  $ep$  and  $e^+e^-$  colliders,” Phys. Rev. D **72**, 115011 (2005) doi:10.1103/PhysRevD.72.115011 [hep-ph/0508205].

- [8] C. R. Chen, W. Klemm, V. Rentala and K. Wang, “Color Sextet Scalars at the CERN Large Hadron Collider,” *Phys. Rev. D* **79**, 054002 (2009) [doi:10.1103/PhysRevD.79.054002](https://doi.org/10.1103/PhysRevD.79.054002) [arXiv:0811.2105 [hep-ph]].
- [9] T. Han, I. Lewis and T. McElmurry, “QCD Corrections to Scalar Diquark Production at Hadron Colliders,” *JHEP* **1001**, 123 (2010) [doi:10.1007/JHEP01\(2010\)123](https://doi.org/10.1007/JHEP01(2010)123) [arXiv:0909.2666 [hep-ph]].
- [10] I. Gogoladze, Y. Mimura, N. Okada and Q. Shafi, “Color Triplet Diquarks at the LHC,” *Phys. Lett. B* **686**, 233 (2010) [doi:10.1016/j.physletb.2010.02.068](https://doi.org/10.1016/j.physletb.2010.02.068) [arXiv:1001.5260 [hep-ph]].
- [11] E. L. Berger, Q. H. Cao, C. R. Chen, G. Shaughnessy and H. Zhang, “Color Sextet Scalars in Early LHC Experiments,” *Phys. Rev. Lett.* **105**, 181802 (2010) [doi:10.1103/PhysRevLett.105.181802](https://doi.org/10.1103/PhysRevLett.105.181802) [arXiv:1005.2622 [hep-ph]].
- [12] T. Han, I. Lewis and Z. Liu, “Colored Resonant Signals at the LHC: Largest Rate and Simplest Topology,” *JHEP* **12**, 085 (2010) [doi:10.1007/JHEP12\(2010\)085](https://doi.org/10.1007/JHEP12(2010)085) [arXiv:1010.4309 [hep-ph]].
- [13] I. Baldes, N. F. Bell and R. R. Volkas, “Baryon Number Violating Scalar Diquarks at the LHC,” *Phys. Rev. D* **84**, 115019 (2011) [doi:10.1103/PhysRevD.84.115019](https://doi.org/10.1103/PhysRevD.84.115019) [arXiv:1110.4450 [hep-ph]].
- [14] P. Richardson and D. Winn, “Simulation of Sextet Diquark Production,” *Eur. Phys. J. C* **72**, 1862 (2012) [doi:10.1140/epjc/s10052-012-1862-z](https://doi.org/10.1140/epjc/s10052-012-1862-z) [arXiv:1108.6154 [hep-ph]].
- [15] D. Karabacak, S. Nandi and S. K. Rai, “Diquark resonance and single top production at the Large Hadron Collider,” *Phys. Rev. D* **85**, 075011 (2012) [doi:10.1103/PhysRevD.85.075011](https://doi.org/10.1103/PhysRevD.85.075011) [arXiv:1201.2917 [hep-ph]].
- [16] M. Kohda, H. Sugiyama and K. Tsumura, “Lepton number violation at the LHC with leptoquark and diquark,” *Phys. Lett. B* **718**, 1436 (2013) [doi:10.1016/j.physletb.2012.12.048](https://doi.org/10.1016/j.physletb.2012.12.048) [arXiv:1210.5622 [hep-ph]].
- [17] R. S. Chivukula, P. Ittisamai, K. Mohan and E. H. Simmons, “Color discriminant variable and scalar diquarks at the LHC,” *Phys. Rev. D* **92**, no. 7, 075020 (2015) [doi:10.1103/PhysRevD.92.075020](https://doi.org/10.1103/PhysRevD.92.075020) [arXiv:1507.06676 [hep-ph]].
- [18] Y. C. Zhan, Z. L. Liu, S. A. Li, C. S. Li and H. T. Li, “Threshold resummation for the production of a color sextet (antitriplet) scalar at the LHC,” *Eur. Phys. J. C* **74**, 2716 (2014) [doi:10.1140/epjc/s10052-014-2716-7](https://doi.org/10.1140/epjc/s10052-014-2716-7) [arXiv:1305.5152 [hep-ph]].
- [19] Z. L. Liu, C. S. Li, Y. Wang, Y. C. Zhan and H. T. Li, “Transverse momentum resummation for color sextet and antitriplet scalar production at the LHC,” *Eur. Phys. J. C* **74**, 2771 (2014) [doi:10.1140/epjc/s10052-014-2771-0](https://doi.org/10.1140/epjc/s10052-014-2771-0) [arXiv:1307.4341 [hep-ph]].
- [20] J. Shu, T. M. P. Tait and K. Wang, “Explorations of the Top Quark Forward-Backward Asymmetry at the Tevatron,” *Phys. Rev. D* **81**, 034012 (2010) [doi:10.1103/PhysRevD.81.034012](https://doi.org/10.1103/PhysRevD.81.034012) [arXiv:0911.3237 [hep-ph]].
- [21] I. Doršner, S. Fajfer, J. F. Kamenik and N. Košnik, “Light colored scalars from grand unification and the forward-backward asymmetry in top quark pair production,” *Phys. Rev. D* **81**, 055009 (2010) [doi:10.1103/PhysRevD.81.055009](https://doi.org/10.1103/PhysRevD.81.055009) [arXiv:0912.0972 [hep-ph]].
- [22] I. Doršner, S. Fajfer, J. F. Kamenik and N. Košnik, “Light Colored Scalar as Messenger of Up-Quark Flavor Dynamics in Grand Unified Theories,” *Phys. Rev. D* **82**, 094015 (2010) [doi:10.1103/PhysRevD.82.094015](https://doi.org/10.1103/PhysRevD.82.094015) [arXiv:1007.2604 [hep-ph]].

- [23] A. Arhrib, R. Benbrik and C. H. Chen, “Forward-backward asymmetry of top quark in diquark models,” *Phys. Rev. D* **82**, 034034 (2010) [doi:10.1103/PhysRevD.82.034034](https://doi.org/10.1103/PhysRevD.82.034034) [arXiv:0911.4875 [hep-ph]].
- [24] Z. Ligeti, G. Marques Tavares and M. Schmaltz, “Explaining the  $t\bar{t}$  forward-backward asymmetry without dijet or flavor anomalies,” *JHEP* **1106**, 109 (2011) [doi:10.1007/JHEP06\(2011\)109](https://doi.org/10.1007/JHEP06(2011)109) [arXiv:1103.2757 [hep-ph]].
- [25] K. Hagiwara and J. Nakamura, “Diquark contributions to Top quark charge asymmetry at the Tevatron and LHC,” *JHEP* **1302**, 100 (2013) [doi:10.1007/JHEP02\(2013\)100](https://doi.org/10.1007/JHEP02(2013)100) [arXiv:1205.5005 [hep-ph]].
- [26] B. C. Allanach and K. Sridhar, “R-Parity Violating Supersymmetry Explanation for Large  $t\bar{t}$  Forward-Backward Asymmetry,” *Phys. Rev. D* **86**, 075016 (2012) [doi:10.1103/PhysRevD.86.075016](https://doi.org/10.1103/PhysRevD.86.075016) [arXiv:1205.5170 [hep-ph]].
- [27] G. Dupuis and J. M. Cline, “Top quark forward-backward asymmetry in R-parity violating supersymmetry,” *JHEP* **1301**, 058 (2013) [doi:10.1007/JHEP01\(2013\)058](https://doi.org/10.1007/JHEP01(2013)058) [arXiv:1206.1845 [hep-ph]].
- [28] C. Han, N. Liu, L. Wu, J. M. Yang and Y. Zhang, “Two-Higgs-doublet model with a color-triplet scalar: a joint explanation for top quark forward-backward asymmetry and Higgs decay to diphoton,” *Eur. Phys. J. C* **73**, no. 12, 2664 (2013) [doi:10.1140/epjc/s10052-013-2664-7](https://doi.org/10.1140/epjc/s10052-013-2664-7) [arXiv:1212.6728 [hep-ph]].
- [29] R. N. Mohapatra and R. E. Marshak, “Local B-L Symmetry of Electroweak Interactions, Majorana Neutrinos and Neutron Oscillations,” *Phys. Rev. Lett.* **44**, 1316 (1980) Erratum: [*Phys. Rev. Lett.* **44**, 1643 (1980)]. [doi:10.1103/PhysRevLett.44.1644.2](https://doi.org/10.1103/PhysRevLett.44.1644.2), [10.1103/PhysRevLett.44.1316](https://doi.org/10.1103/PhysRevLett.44.1316)
- [30] K. S. Babu, P. S. Bhupal Dev and R. N. Mohapatra, “Neutrino mass hierarchy, neutron - anti-neutron oscillation from baryogenesis,” *Phys. Rev. D* **79**, 015017 (2009) [doi:10.1103/PhysRevD.79.015017](https://doi.org/10.1103/PhysRevD.79.015017) [arXiv:0811.3411 [hep-ph]].
- [31] M. A. Ajaib, I. Gogoladze, Y. Mimura and Q. Shafi, “Observable  $n-\bar{n}$  Oscillations with New Physics at LHC,” *Phys. Rev. D* **80**, 125026 (2009) [doi:10.1103/PhysRevD.80.125026](https://doi.org/10.1103/PhysRevD.80.125026) [arXiv:0910.1877 [hep-ph]].
- [32] P. H. Gu and U. Sarkar, “Baryogenesis and neutron-antineutron oscillation at TeV,” *Phys. Lett. B* **705**, 170 (2011) [doi:10.1016/j.physletb.2011.10.017](https://doi.org/10.1016/j.physletb.2011.10.017) [arXiv:1107.0173 [hep-ph]].
- [33] K. S. Babu and R. N. Mohapatra, “Coupling Unification, GUT-Scale Baryogenesis and Neutron-Antineutron Oscillation in SO(10),” *Phys. Lett. B* **715**, 328 (2012) [doi:10.1016/j.physletb.2012.08.006](https://doi.org/10.1016/j.physletb.2012.08.006) [arXiv:1206.5701 [hep-ph]].
- [34] J. M. Arnold, B. Fornal and M. B. Wise, “Simplified models with baryon number violation but no proton decay,” *Phys. Rev. D* **87**, 075004 (2013) [doi:10.1103/PhysRevD.87.075004](https://doi.org/10.1103/PhysRevD.87.075004) [arXiv:1212.4556 [hep-ph]].
- [35] K. S. Babu, P. S. Bhupal Dev, E. C. F. S. Fortes and R. N. Mohapatra, “Post-Sphaleron Baryogenesis and an Upper Limit on the Neutron-Antineutron Oscillation Time,” *Phys. Rev. D* **87**, no. 11, 115019 (2013) [doi:10.1103/PhysRevD.87.115019](https://doi.org/10.1103/PhysRevD.87.115019) [arXiv:1303.6918 [hep-ph]].
- [36] N. B. Beaudry, A. Datta, D. London, A. Rashed and J. S. Roux, “The  $B \rightarrow \pi K$  puzzle revisited,” *JHEP* **1801**, 074 (2018) [doi:10.1007/JHEP01\(2018\)074](https://doi.org/10.1007/JHEP01(2018)074) [arXiv:1709.07142 [hep-ph]].

- [37] C. H. Chen and T. Nomura, “Left-handed color-sextet diquark in the Kaon system,” *Phys. Rev. D* **99**, no. 11, 115006 (2019) [doi:10.1103/PhysRevD.99.115006](https://doi.org/10.1103/PhysRevD.99.115006) [arXiv:1811.02315 [hep-ph]].
- [38] P. B. Dev, R. Mohanta, S. Patra and S. Sahoo, “Unified explanation of flavor anomalies, radiative neutrino mass and ANITA anomalous events in a vector leptoquark model,” [arXiv:2004.09464 [hep-ph]].
- [39] G. F. Giudice, B. Gripaios and R. Sundrum, “Flavourful Production at Hadron Colliders,” *JHEP* **1108**, 055 (2011) [doi:10.1007/JHEP08\(2011\)055](https://doi.org/10.1007/JHEP08(2011)055) [arXiv:1105.3161 [hep-ph]].
- [40] G. Bhattacharyya, D. Choudhury and K. Sridhar, “New LEP bounds on  $B$  violating scalar couplings: R-parity violating supersymmetry or diquarks,” *Phys. Lett. B* **355**, 193 (1995) [doi:10.1016/0370-2693\(95\)00701-L](https://doi.org/10.1016/0370-2693(95)00701-L) [hep-ph/9504314].
- [41] E. C. F. S. Fortes, K. S. Babu and R. N. Mohapatra, “Flavor Physics Constraints on TeV Scale Color Sextet Scalars,” [arXiv:1311.4101 [hep-ph]].
- [42] For example, see N. Assad, B. Fornal and B. Grinstein, “Baryon Number and Lepton Universality Violation in Leptoquark and Diquark Models,” *Phys. Lett. B* **777**, 324-331 (2018) [doi:10.1016/j.physletb.2017.12.042](https://doi.org/10.1016/j.physletb.2017.12.042) [arXiv:1708.06350 [hep-ph]].
- [43] A. M. Sirunyan *et al.* [CMS], “Search for narrow and broad dijet resonances in proton-proton collisions at  $\sqrt{s} = 13$  TeV and constraints on dark matter mediators and other new particles,” *JHEP* **08**, 130 (2018) [doi:10.1007/JHEP08\(2018\)130](https://doi.org/10.1007/JHEP08(2018)130) [arXiv:1806.00843 [hep-ex]].
- [44] J. Alwall, R. Frederix, S. Frixione, V. Hirschi, F. Maltoni, O. Mattelaer, H. S. Shao, T. Stelzer, P. Torrielli and M. Zaro, “The automated computation of tree-level and next-to-leading order differential cross sections, and their matching to parton shower simulations,” *JHEP* **07**, 079 (2014) [doi:10.1007/JHEP07\(2014\)079](https://doi.org/10.1007/JHEP07(2014)079) [arXiv:1405.0301 [hep-ph]].
- [45] A. Alloul, N. D. Christensen, C. Degrande, C. Duhr and B. Fuks, “FeynRules 2.0 - A complete toolbox for tree-level phenomenology,” *Comput. Phys. Commun.* **185**, 2250-2300 (2014) [doi:10.1016/j.cpc.2014.04.012](https://doi.org/10.1016/j.cpc.2014.04.012) [arXiv:1310.1921 [hep-ph]].
- [46] J. Alwall, C. Duhr, Triplet diquark model, <https://feynrules.irmp.ucl.ac.be/wiki/Triplets>.
- [47] J. Pumplin, D. Stump, J. Huston, H. Lai, P. M. Nadolsky and W. Tung, “New generation of parton distributions with uncertainties from global QCD analysis,” *JHEP* **07**, 012 (2002) [doi:10.1088/1126-6708/2002/07/012](https://doi.org/10.1088/1126-6708/2002/07/012) [arXiv:hep-ph/0201195 [hep-ph]].
- [48] For a model-independent study of constraints on NP from STP, see D. Stolarski and A. Toner, “Constraining New Physics with Single Top production at LHC,” [arXiv:2004.07856 [hep-ph]].
- [49] M. Aaboud *et al.* [ATLAS], “Fiducial, total and differential cross-section measurements of  $t$ -channel single top-quark production in  $pp$  collisions at 8 TeV using data collected by the ATLAS detector,” *Eur. Phys. J. C* **77**, no. 8, 531 (2017) [doi:10.1140/epjc/s10052-017-5061-9](https://doi.org/10.1140/epjc/s10052-017-5061-9) [arXiv:1702.02859 [hep-ex]].
- [50] A. M. Sirunyan *et al.* [CMS], “Measurement of the single top quark and antiquark production cross sections in the  $t$  channel and their ratio in proton-proton collisions at  $\sqrt{s} = 13$  TeV,” *Phys. Lett. B* **800**, 135042 (2020) [doi:10.1016/j.physletb.2019.135042](https://doi.org/10.1016/j.physletb.2019.135042) [arXiv:1812.10514 [hep-ex]].

- [51] LHC Top Working Group,  
<https://twiki.cern.ch/twiki/bin/view/LHCPhysics/LHCTopWGSummaryPlots>.
- [52] ATLAS-CMS recommended predictions for single-top cross sections using the Hathor v2.1 program, <https://twiki.cern.ch/twiki/bin/view/LHCPhysics/SingleTopRefXsec>.
- [53] M. Aliev, H. Lacker, U. Langenfeld, S. Moch, P. Uwer and M. Wiedermann, “HATHOR: HAdronic Top and Heavy quarks crOss section calculatoR,” *Comput. Phys. Commun.* **182**, 1034-1046 (2011) [doi:10.1016/j.cpc.2010.12.040](https://doi.org/10.1016/j.cpc.2010.12.040) [arXiv:1007.1327 [hep-ph]].
- [54] P. Kant, O. Kind, T. Kintscher, T. Lohse, T. Martini, S. Mlbitz, P. Rieck and P. Uwer, “HatHor for single top-quark production: Updated predictions and uncertainty estimates for single top-quark production in hadronic collisions,” *Comput. Phys. Commun.* **191**, 74-89 (2015) [doi:10.1016/j.cpc.2015.02.001](https://doi.org/10.1016/j.cpc.2015.02.001) [arXiv:1406.4403 [hep-ph]].
- [55] M. Botje, J. Butterworth, A. Cooper-Sarkar, A. de Roeck, J. Feltesse, S. Forte, A. Glazov, J. Huston, R. McNulty, T. Sjostrand and R. Thorne, “The PDF4LHC Working Group Interim Recommendations,” [arXiv:1101.0538 [hep-ph]].
- [56] A. Martin, W. Stirling, R. Thorne and G. Watt, “Parton distributions for the LHC,” *Eur. Phys. J. C* **63**, 189-285 (2009) [doi:10.1140/epjc/s10052-009-1072-5](https://doi.org/10.1140/epjc/s10052-009-1072-5) [arXiv:0901.0002 [hep-ph]].
- [57] A. Martin, W. Stirling, R. Thorne and G. Watt, “Uncertainties on  $\alpha_S$  in global PDF analyses and implications for predicted hadronic cross sections,” *Eur. Phys. J. C* **64**, 653-680 (2009) [doi:10.1140/epjc/s10052-009-1164-2](https://doi.org/10.1140/epjc/s10052-009-1164-2) [arXiv:0905.3531 [hep-ph]].
- [58] H. L. Lai, M. Guzzi, J. Huston, Z. Li, P. M. Nadolsky, J. Pumplin and C. P. Yuan, “New parton distributions for collider physics,” *Phys. Rev. D* **82**, 074024 (2010) [doi:10.1103/PhysRevD.82.074024](https://doi.org/10.1103/PhysRevD.82.074024) [arXiv:1007.2241 [hep-ph]].
- [59] R. D. Ball, V. Bertone, S. Carrazza, C. S. Deans, L. Del Debbio, S. Forte, A. Guffanti, N. P. Hartland, J. I. Latorre, J. Rojo and M. Ubiali, “Parton distributions with LHC data,” *Nucl. Phys. B* **867**, 244-289 (2013) [doi:10.1016/j.nuclphysb.2012.10.003](https://doi.org/10.1016/j.nuclphysb.2012.10.003) [arXiv:1207.1303 [hep-ph]].
- [60] The ATLAS Collaboration, private communication.